

## Article

# Analyses of Sulfur and Iron in Waterlogged Archaeological Wood: The Case of Polyethylene-Glycol-Treated Yenikapı 12 Shipwreck

Aslı Gökçe Kılıç<sup>1,\*</sup> , Namık Kılıç<sup>2</sup>  and Donna C. Arnold<sup>3</sup> 

<sup>1</sup> Museology Department, Faculty of Letters, Istanbul University, Fatih, 34134 Istanbul, Türkiye

<sup>2</sup> Department of Conservation of Marine Archaeological Objects, Faculty of Letters, Istanbul University, Fatih, 34134 Istanbul, Türkiye

<sup>3</sup> School of Chemistry and Forensic Science, Division of Natural Sciences Canterbury, University of Kent, Kent CT2 7NH, UK

\* Correspondence: gokcegokcay@istanbul.edu.tr

**Abstract:** The Yenikapı (YK) 12 shipwreck is 1 of 37 shipwrecks found at Yenikapı, Istanbul. This merchantman has been dated to AD 672–876 by radiocarbon analyses. The conservation of YK 12, which was assembled with iron nails, was completed with the pre-impregnation of polyethylene glycol (PEG) and using vacuum freeze-drying processes. However, after conservation, dust formation was observed on some wooden parts of the shipwreck during storage. In this study, iron–sulfur-related problems detected in the woods of YK 12 were evaluated. We analysed samples taken from YK 12 to study the sulfur and iron content in woods from oak (*Quercus*), walnut (*Juglans*), and hornbeam (*Carpinus*), representing taxa with different wood properties. Fourier-transform infrared spectroscopy (FTIR) analyses, X-ray diffraction (XRD), and pH measurements were conducted on five samples. The results of these studies showed that the dust consisted of wood particles, PEG, and hydrated iron sulfates, such as  $\text{FeSO}_4 \cdot 4\text{H}_2\text{O}$  and  $\text{FeSO}_4 \cdot 7\text{H}_2\text{O}$ . Additionally, one sample included  $\text{SiO}_2$ , whilst another exhibited a low pH value. These findings highlight the importance of optimum ambient conditions for the storage and display of these shipwrecks in order to prevent the irreversible degradation of YK 12 and other recovered shipwrecks.

**Keywords:** waterlogged archaeological wood; Yenikapı shipwrecks; XRD; FTIR; pH; sulfur; iron



**Citation:** Kılıç, A.G.; Kılıç, N.; Arnold, D.C. Analyses of Sulfur and Iron in Waterlogged Archaeological Wood: The Case of Polyethylene-Glycol-Treated Yenikapı 12 Shipwreck. *Forests* **2023**, *14*, 530. <https://doi.org/10.3390/f14030530>

Academic Editor: Magdalena Broda

Received: 27 January 2023

Revised: 2 March 2023

Accepted: 6 March 2023

Published: 8 March 2023



**Copyright:** © 2023 by the authors. Licensee MDPI, Basel, Switzerland. This article is an open access article distributed under the terms and conditions of the Creative Commons Attribution (CC BY) license (<https://creativecommons.org/licenses/by/4.0/>).

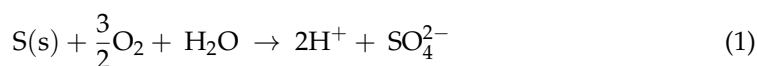
## 1. Introduction

Scientific studies have been conducted on the conservation of waterlogged archaeological wood since the 1860s. However, the conservation process of waterlogged archaeological wood remains challenging due to the long timeframes and high cost of these processes, especially given the enormous size of shipwrecks. The solutions of alum salts ( $\text{KAl}(\text{SO}_4)_2 \cdot 12\text{H}_2\text{O}$ ) were used for the conservation of waterlogged archaeological wood for the first time in the mid-1800s [1,2]. More recently, PEG (polyethylene glycol) with different molecular weights is one of the most utilised methods for conserving waterlogged archaeological wood. However, the use of PEG introduces problems with respect to conservation, for example, acidity formation in wood, which leads to degradation. In the 1970s, white powder deposits were detected, due to the acidity, in the woods of the Skuldelev shipwrecks treated with PEG. After analyses, these powders were identified as hydrated iron sulfate particles resulting from the oxidation of insoluble iron sulfides. Similar powder formation was also detected in wood samples from the Vasa shipwreck. As a result, this was defined as a significant problem for the conservation of waterlogged wood in the 2000s due to high sulfur contents in the recovered materials [3–7].

Iron corrosion products found in marine archaeological woods are caused by iron nails and objects (e.g., cannons and cannon balls), which sunk with the ship. In anoxic

environments with low redox potentials, H<sub>2</sub>S can be enriched by sulphate-reducing bacteria (SRB). Iron sulfides can then be produced in the presence of iron. Typically, sulfur accumulation is exclusively associated with anaerobic conditions. However, aerobic or fluctuating oxygen levels can promote sulfur deposition in waterlogged archaeological wood [8,9]. Sulfur accumulated in the woods from shipwrecks affects the conservation process and long-term stability of the timbers [10,11]. Therefore, archaeological woods need to be monitored carefully during display and storage.

Additionally, reduced sulfur compounds may transform into sulfuric acid when the relative humidity in the area where the woods are located is high. Furthermore, it has been found that iron nails/objects act as catalysts for the acidity formation reaction. Numerous instrumental analyses are used to determine sulfur–iron compounds in waterlogged archaeological wood. XRD (X-ray diffraction) can be used when crystalline salt deposits form on the wood. In addition, Raman spectroscopy and portable XRF (X-ray fluorescence spectroscopy) can detect iron–sulfur compounds in wood. SEM-EDX (scanning electron microscope energy-dispersive X-ray spectroscopy) can map sulfur and iron distribution in the wood cell wall alongside providing morphological information. XPS (X-ray photoelectron spectrometry) and XANES (X-ray absorption near edge spectroscopy) can identify the valences of sulfur and iron, providing further confirmation for the phases formed, and SXM (scanning X-ray spectro-microscopy) can evaluate the microscopic sulfur compounds in the wood [6,9,11–17]. More recently, magnetic measurements have been used to analyse iron–sulfur compounds in waterlogged archaeological wood [18], whereby magnetic behaviour can be used to identify the iron phases present from their characteristic magnetic behaviour. Iron compounds are widely found in the woods of shipwrecks treated with PEG. SEM–EDX and XAFS analyses on the wood of the Swedish Vasa shipwreck showed that FeSO<sub>4</sub>·7H<sub>2</sub>O, KFe<sub>3</sub>(SO<sub>4</sub>)<sub>2</sub>(OH)<sub>6</sub>, NaFe<sub>3</sub>(SO<sub>4</sub>)<sub>2</sub>(OH)<sub>6</sub>, and CaSO<sub>4</sub> compounds had accumulated. SEM, XANES, XRD, and EXAFS analyses of the wood from the Mary Rose shipwreck from the United Kingdom demonstrated the presence of FeS<sub>2</sub>, Fe<sub>8</sub>S<sub>9</sub>, Fe<sub>2</sub>O<sub>3</sub>, FeSO<sub>4</sub>·4H<sub>2</sub>O, FeSO<sub>4</sub>·7H<sub>2</sub>O, NaFe<sub>3</sub>(SO<sub>4</sub>)<sub>2</sub>(OH)<sub>6</sub>, KFe<sub>3</sub>(SO<sub>4</sub>)<sub>2</sub>(OH)<sub>6</sub>, CaSO<sub>4</sub>·2H<sub>2</sub>O, and CaCO<sub>3</sub> compounds [19–21]. Likewise, XRD analysis of wood samples from the Batavia shipwreck from Australia also confirmed the presence of FeS, FeS<sub>2</sub>, FeOOH, Fe(OH)<sub>2</sub>, FeSO<sub>4</sub>·4H<sub>2</sub>O, FeSO<sub>4</sub>·5H<sub>2</sub>O, KFe<sub>3</sub>(SO<sub>4</sub>)<sub>2</sub>(OH)<sub>6</sub>, and NaFe<sub>3</sub>(SO<sub>4</sub>)<sub>2</sub>(OH)<sub>6</sub> compounds [22,23]. Unusually, SEM-EDX, micro-Raman spectroscopy (μ-RS), and XRD analyses of wood samples taken from the Lyon Saint-Georges 4 (from France) only showed the presence of FeS<sub>2</sub> and Fe<sub>3</sub>S<sub>4</sub> phases [24]. Lastly, XRD analysis of the Shinan shipwreck from South Korea showed similar phases to those found in the shipwrecks discussed above, namely, S, FeS<sub>2</sub>, FeSO<sub>4</sub>·5H<sub>2</sub>O, FeSO<sub>4</sub>·7H<sub>2</sub>O, KFe<sub>3</sub>(SO<sub>4</sub>)<sub>2</sub>(OH)<sub>6</sub>, FeO·OH, CaSO<sub>4</sub>·2H<sub>2</sub>O, AlSi<sub>0.5</sub>O<sub>2.5</sub>, Na<sub>2</sub>SiF<sub>6</sub>, Na<sub>2</sub>B<sub>4</sub>O<sub>5</sub>(OH)<sub>4</sub>·2H<sub>2</sub>O, and SiO<sub>2</sub> [25–27]. Alongside instrumental methods, pH measurements are also used to determine the acidity of archaeological samples [28]. The Vasa, Mary Rose, and Batavia shipwrecks treated with PEG all exhibit acidity problems in the woods [29,30]. The acidity formation process is shown by Equations (1) and (2) [25,31]:



The information obtained from these shipwrecks motivates the continued studies of more recently uncovered marine archaeological finds. One such significant group is the Yenikapı shipwrecks, which were uncovered under the supervision of the Istanbul Archaeology Museums Directorate between 2004 and 2013. These 37 shipwrecks, dated to the medieval era, are considered the world’s largest medieval shipwreck collection [32]. The conservation work on 31 of these 37 shipwrecks has been implemented by the Istanbul University (İÜ)’s Department of Conservation of Marine Archaeological Objects within the İÜ Yenikapı Shipwrecks Project. The project performs the conservation of most shipwrecks using pre-impregnation with polyethylene glycol and the application of vacuum freeze-

drying. Furthermore, with the knowledge of the acidity problem due to iron–sulfur compounds, the iron corrosion parts of the woods are cleaned mechanically and chemically.

This study focuses on the YK (Yenikapı) 12 shipwreck (Figure 1). YK 12 is a merchantman, which was excavated with its cargo of amphoras. In addition, in a separate compartment at the stern, personal belongings, possibly those of the captain, were found. The coins found with the YK 12 shipwreck date it to the 9th century using radiocarbon analyses, providing a date range of AD 672–876. The shipwreck’s extant length is 7 m, and its width is 2.3 m. The ship’s planks were fixed to the floor timbers using iron nails [33,34].



**Figure 1.** Photo of the Yenikapı 12 shipwreck (© IU Yenikapı Shipwrecks Project Archive).

The desalination of the YK 12 shipwreck was made in stainless steel tanks at the İU Yenikapı Shipwrecks Research Laboratory. The salinity content of these tanks was measured at approximately 1000 ppm. This value was decreased to approximately 40 ppm using tap and distilled water over a timeframe of almost one year. During the desalination process, the preservative agent, isothiazolone, was added to the tank at concentrations of 0.1% to protect against biological activity. Coordinating with the desalination process, iron corrosion parts in the woods (e.g., nails) were cleaned. Firstly, the woods were cleaned mechanically. After mechanical cleaning, these areas were buffered three times with a 5% disodium EDTA solution, and then, the woods were neutralised in distilled water. The PEG impregnation process of the YK 12 shipwreck was made in the same stainless steel tanks at the İU Yenikapı Shipwrecks Research Laboratory. The concentration of the PEG 2000 solution was gradually increased from 10% to 30%. Then, PEG 3000 was impregnated into the woods. The concentration of the PEG 3000 solution was gradually increased by 30% to reach a final concentration of 45%. The impregnation process took four years. Following the pre-impregnation process, the woods were dried using the freeze-drying method [35]. The treated woods are stored at the İU Yenikapı Shipwrecks Research Laboratory. In this paper, we report the results of the analyses conducted on the woods of YK 12 while monitoring during storage.

## 2. Materials and Methods

### 2.1. Sampling

While storing the PEG-treated archaeological woods of the YK 12 shipwreck, dust formation was observed on some of the timbers. These wooden parts are from the frame of the shipwreck and are named E8, E9, E11, E13, and E17 (Figure 2). Five dust samples were collected from these areas and were analysed using FTIR and XRD. Additionally, wood samples were collected from the same sample group (E8, E9, E11, E13, and E17) for FTIR analyses. In order to compare the spectra collected for the PEG-treated archaeological wood samples, fresh wood samples from the same species as the archaeological wood samples were also analysed by FTIR (Table 1). Prior to FTIR analysis, the fresh wood samples—oak (*Quercus*), walnut (*Juglans*), and hornbeam (*Carpinus*)—were dried in an oven at  $100 \pm 2$  °C.

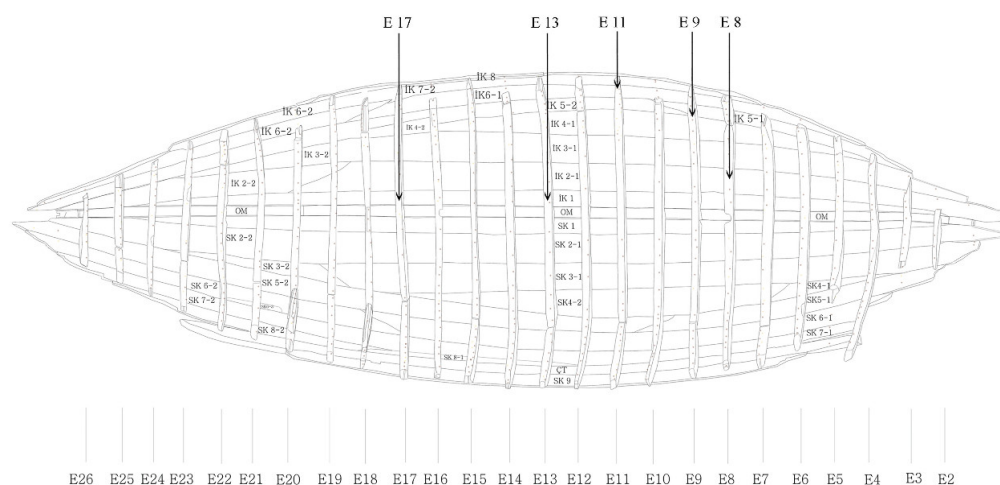


**Figure 2.** Schematic representation of the YK 12 shipwreck showing the sampling points denoted E8, E9, E11, E13, and E17 (I. Özsait-Kocabaş).

**Table 1.** Wood species of the wood samples taken at the sampling points E8, E9, E11, E13, and E17.

Sample	Species
E8	Hornbeam ( <i>Carpinus</i> )
E9	Oak ( <i>Quercus</i> )
E11	Oak ( <i>Quercus</i> )
E13	Walnut ( <i>Juglans</i> )
E17	Oak ( <i>Quercus</i> )

Key to symbol; E: frame.

## 2.2. FTIR Analyses

FTIR spectroscopy was carried out using a Perkin Elmer Spectrum One series FTIR spectrometer. The spectra were collected (16 scans/sample) between 4000 and 600  $\text{cm}^{-1}$  at a resolution of 4  $\text{cm}^{-1}$ .

## 2.3. XRD Analyses

XRD analyses were performed to determine the crystal structure and phase identification of the dust samples. Data were collected on a Rigaku miniflex 600 diffractometer (20 kV, 15 mA,  $\lambda = 1.5406 \text{ \AA}$ ) over a two-theta range of 5° to 70° with a step size of 0.02° and a run time of approximately 6 h. Data analysis was performed using Highscore software equipped with the JCPDS (Joint Committee of Powder Diffraction Standards) database for search–match functionality.

## 2.4. pH Measurement

Non-destructive pH measurements were carried out using wetted pH strips pressed to the surface of the woods of E8, E9, E11, E13, and E17 [36]. Multiple pH measurements were conducted in the area where dust occurred.

## 3. Results and Discussion

Visual inspections of the FTIR spectra collected for the dust and wood samples and pure PEG were evaluated to determine their similarities. In the spectra collected for the E8 and E17 dust samples, symmetrical C-O-C stretching was observed at  $\sim 841 \text{ cm}^{-1}$ . This band is specific for PEG [37,38]. Therefore, it can be concluded that the dust samples contained PEG. In addition, the spectra of the dust samples and wood samples taken from the E8 and E17 positions exhibited very similar patterns in the range of 1800–800  $\text{cm}^{-1}$  (fingerprint region) [39], suggesting that the dust samples also contained wooden parts (Figure 3).

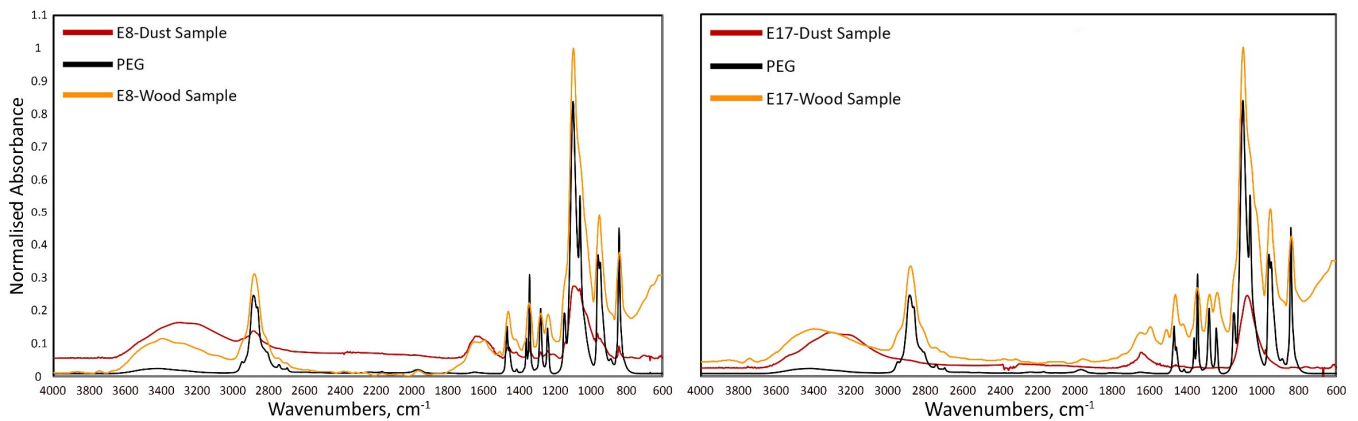


**Figure 3.** FTIR spectra collected for the E8 and E17 dust samples, PEG, and archaeological wood samples.

Furthermore, the spectra collected for the dust samples of E9, E11, and E13 show numerous similar peaks in the region between 1500 and 800  $\text{cm}^{-1}$ , suggesting the presence of both PEG and wooden parts in the samples is consistent with the data collected for E8 and E17 (Figure 4).

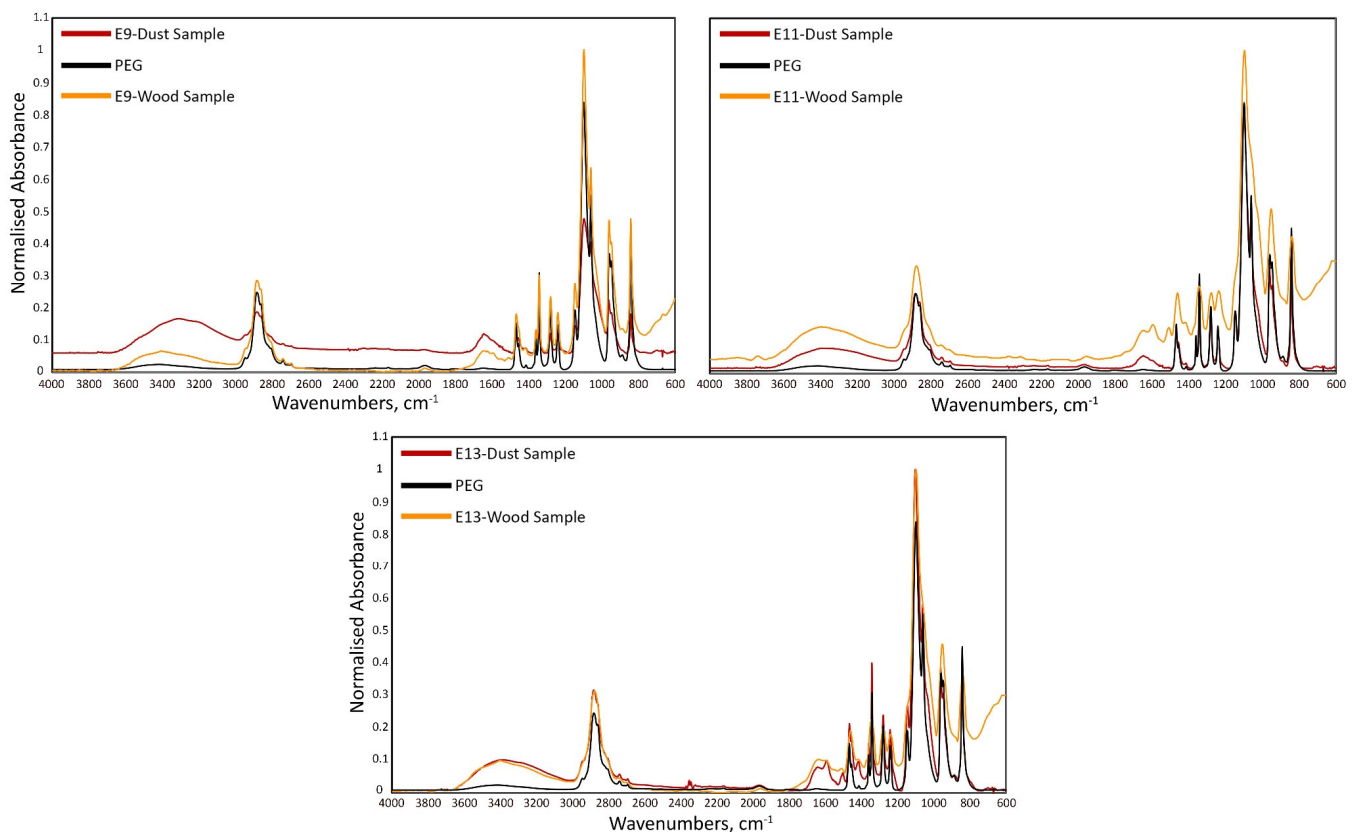


**Figure 4.** FTIR spectra collected for the E9, E11, and E13 dust samples, PEG, and archaeological wood samples.

Analysis of the FTIR spectra collected for the wood samples showed similar trends to those collected for the dust collections. Figure 5 shows a comparison between the spectra collected for the E8 (hornbeam), PEG, and fresh hornbeam samples. The vibration bands at  $\sim 1465$ , 1340, 1278, 1242, 1100, 960, and 841  $\text{cm}^{-1}$  (labelled D to J, respectively) are common across all spectra collected. The band at  $\sim 1732$   $\text{cm}^{-1}$  (labelled A) is associated with unconjugated carbonyl stretching in hemicelluloses [40], as shown in the spectrum

collected for the fresh hornbeam wood sample. However, no peak can be observed in the corresponding spectrum collected for the wood sample, E8. This suggests hemicellulose degradation in the wood sample. The vibration bands at  $\sim 1502\text{ cm}^{-1}$  and  $\sim 1592\text{ cm}^{-1}$  (labelled B) belong to lignin [41,42]. This peak can also be observed in both the spectra collected for the fresh wood and the archaeological wood samples.

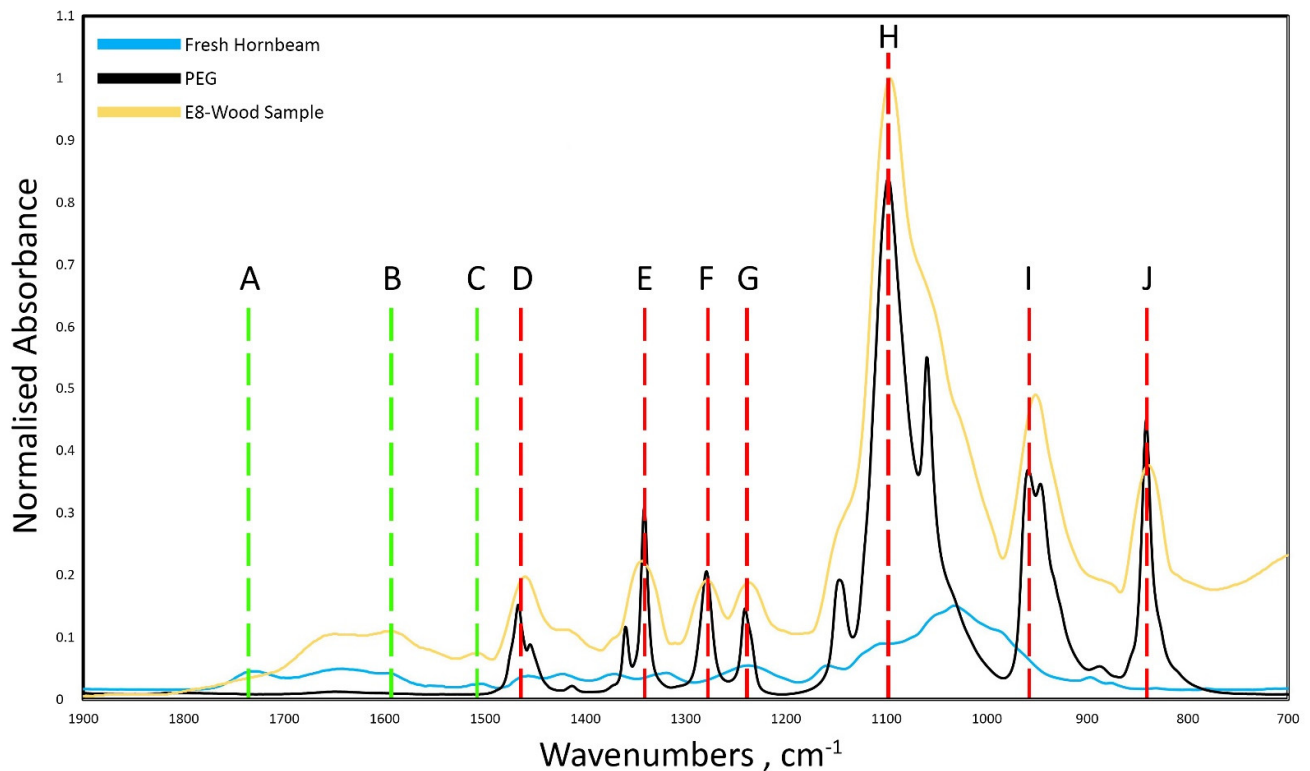


**Figure 5.** FTIR spectra collected for fresh hornbeam, PEG, and the wood sample collected at the E8 site.

In contrast with E8 (hornbeam), the species associated with the E9, E11, and E17 wood samples is oak. A comparison of these samples with fresh oak and PEG samples is shown in Figure 6. Similarly to the E8 wood sample, both the PEG and archaeological wood samples exhibit vibration bands at  $\sim 1465$ ,  $1340$ ,  $1278$ ,  $1242$ ,  $1144$ ,  $1100$ ,  $960$ , and  $841\text{ cm}^{-1}$  (labelled D to K, respectively), which are consistent with the presence of PEG. Additionally, vibration bands at  $\sim 1732\text{ cm}^{-1}$  (labelled A),  $\sim 1592\text{ cm}^{-1}$  (labelled B), and  $\sim 1502\text{ cm}^{-1}$  (labelled C) can be observed in the fresh oak samples and can be identified as arising from hemicellulose and lignin respectively. As with the E8 hornbeam wood sample, hemicellulose cannot be observed in the spectra collected for the E9, E11, and E17 wood samples, again suggesting the degradation of these samples. Moreover, the intensity of lignin peaks can be seen to decrease in the spectrum collected for the E9 sample, suggesting lignin degradation also occurred.

Lastly, the same comparisons were made for the spectra collected for the E13 walnut wood sample with fresh walnut and PEG samples. The FTIR spectra collected are shown in Figure 7. As seen for the other samples, the bands at  $\sim 1465$ ,  $1340$ ,  $1278$ ,  $1242$ ,  $1100$ ,  $960$ , and  $841\text{ cm}^{-1}$  (labelled from D to J, respectively) are common across both the spectra of the wood sample and PEG. Additionally, the vibration bands at  $\sim 1636\text{ cm}^{-1}$ ,  $\sim 1592\text{ cm}^{-1}$ , and  $\sim 1502\text{ cm}^{-1}$  (labelled A to C) belong to lignin [41,42]. Interestingly, there is no evidence for hemicelluloses in either wood sample (fresh or archaeological).

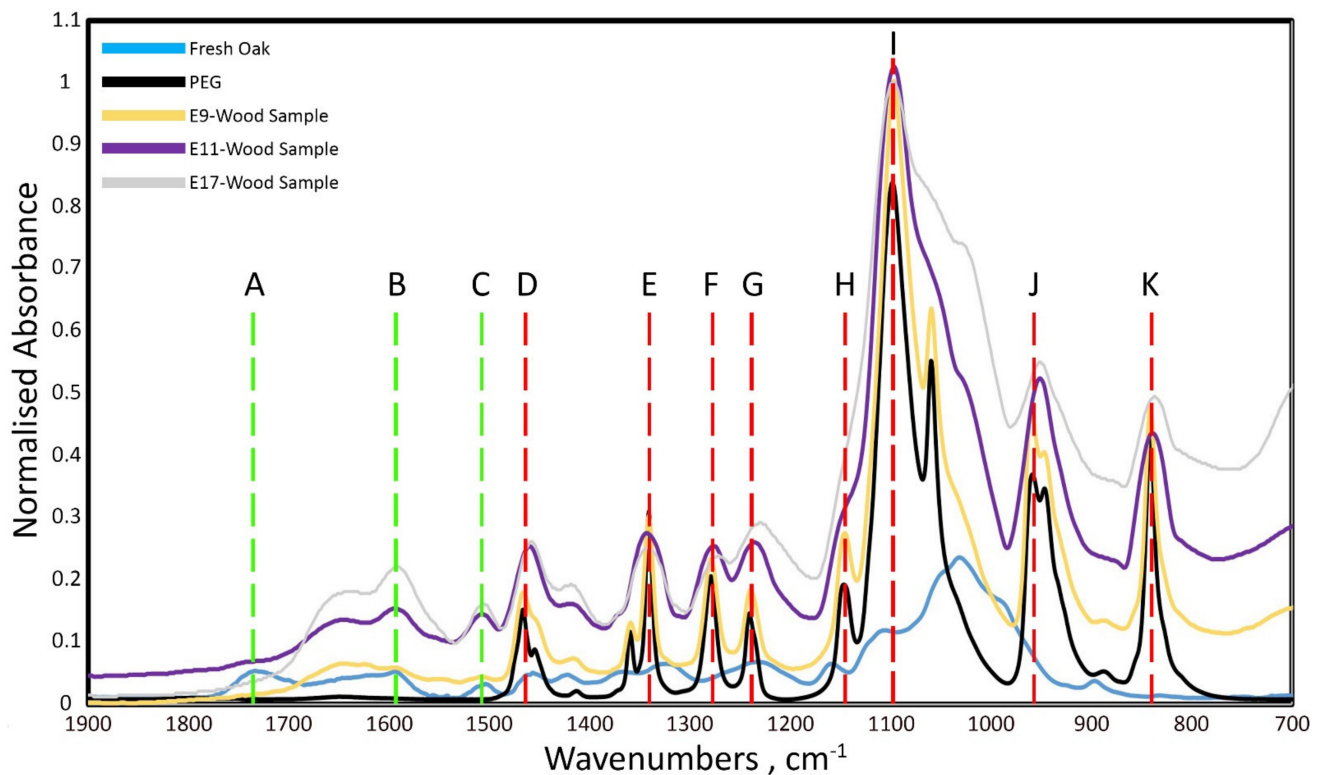


Figure 6. FTIR spectra collected for fresh oak, PEG, and the E9, E11, and E17 archaeological wood samples.

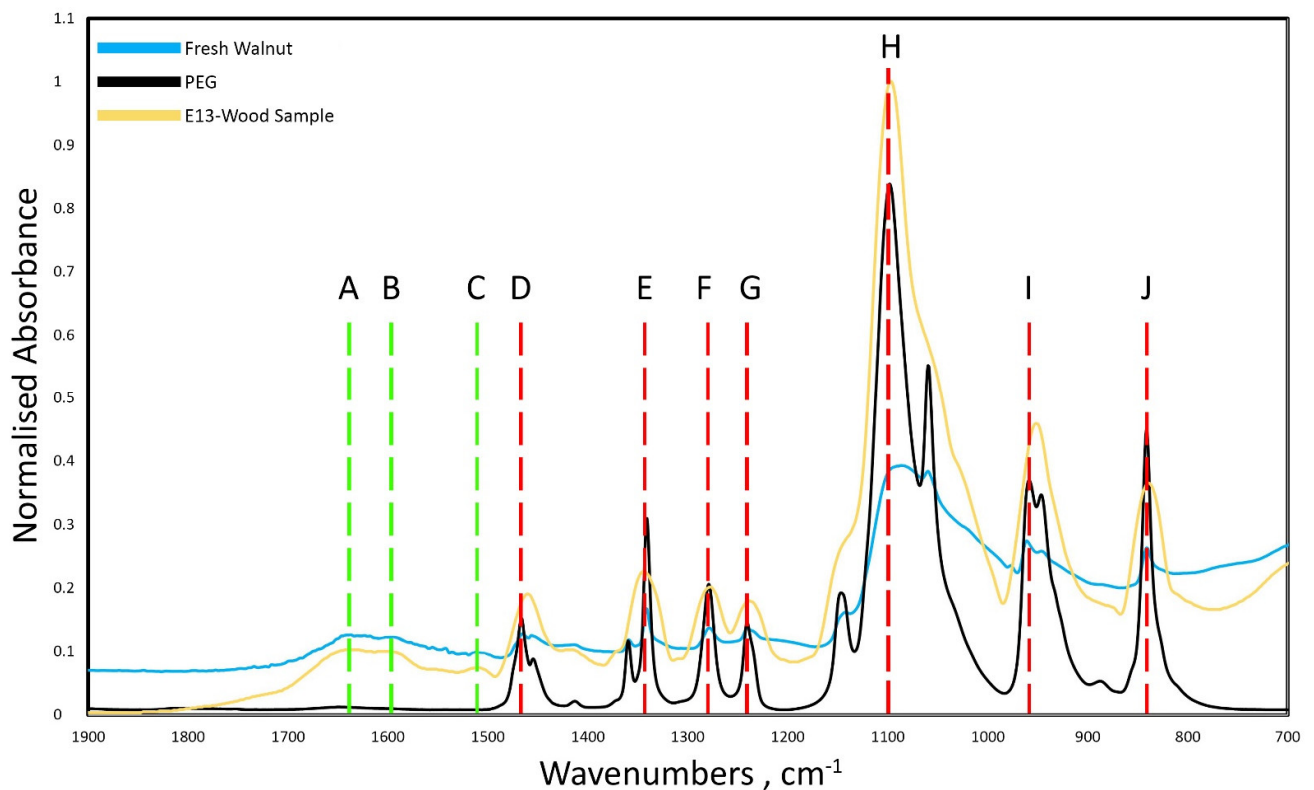
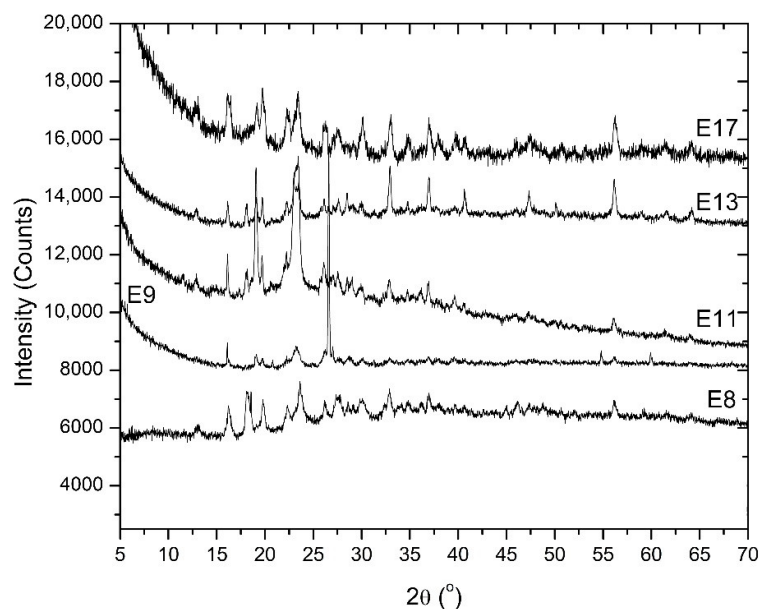


Figure 7. FTIR spectra collected for fresh walnut, PEG, and the E13 archaeological wood sample.

The XRD measurements revealed the presence of salts, which may have precipitated during the drying of the woods [43]. The comparison plot of the data collected for the dust samples is shown in Figure 8. There are some similarities between the X-ray diffraction data

collected. The E8, E13, and E17 samples show very similar diffraction patterns, suggesting that they largely contain the same phases. Sample E11 shows similarities to the other diffraction patterns. However, in E11, the differences are mostly in the peak intensity ratios, suggesting that the same components are present but that they are present in different quantities. In contrast, E9 exhibits a very different pattern, suggesting that the main phase contributions to the diffraction pattern come from an alternative source.



**Figure 8.** Comparison plot of the X-ray diffraction data collected for the dust samples collected for E8, E9, E11, E13, and E17. Patterns are shifted for clarity, and E17 is enhanced by a factor of 4 to allow comparisons.

The peak positions and intensities of the samples were searched for possible matches in the JCPDS database. This allowed us to determine the crystalline phases present in these materials in more detail. Table 2 provides a summary of the search–match results observed for each of the dust samples.

**Table 2.** Search–match results from the X-ray diffraction data collected for the E8, E9, E11, E13, and E17 dust samples.

Sample	Primary Phase	Secondary Phase
E8	FeSO <sub>4</sub> ·4H <sub>2</sub> O	FeSO <sub>4</sub> ·7H <sub>2</sub> O
E9	SiO <sub>2</sub>	FeSO <sub>4</sub> ·4H <sub>2</sub> O
E11	FeSO <sub>4</sub> ·4H <sub>2</sub> O	FeSO <sub>4</sub> ·7H <sub>2</sub> O
E13	FeSO <sub>4</sub> ·4H <sub>2</sub> O	FeSO <sub>4</sub> ·7H <sub>2</sub> O
E17	FeSO <sub>4</sub> ·4H <sub>2</sub> O	FeSO <sub>4</sub> ·7H <sub>2</sub> O

E8, E11, E13, and E17 showed a mixture of two hydrated iron sulfate phases—rozenite (FeSO<sub>4</sub>·4H<sub>2</sub>O) and melanterite (FeSO<sub>4</sub>·7H<sub>2</sub>O)—which suggests that these sulfate phases are hydrated over time. In contrast, the pattern collected for E9 is dominated by quartz (SiO<sub>2</sub>), with a much smaller contribution from the rozenite phase. Pyrite was not detected in the dust samples. However, it should be noted that this may be present in small quantities that are beneath the limit of detection for the instrument or masked by peak overlap. Previous studies conducted on waterlogged archaeological wood have mentioned the presence of sulfur, pyrite, and traces of mackinawite. However, these studies have additionally mentioned the presence of iron/sulfate-containing compounds, mainly hydrated iron sulfates (rozenite and melanterite), consistent with the observations in this work. In

addition, sulfated phases such as rozenite and melanterite could be detected at the surface of the woods. Therefore, the formation of rozenite and melanterite could be caused by the precipitation of sulfate with iron species during the drying of the wood. Moreover, the formation of the rozenite and melanterite salts on the surface of the wood can also arise as a result of the degradation products from cellulose and formic acid, which can reduce iron (III) ions [44,45].

To determine the acidity of the woods in which dust formed, their pH values were measured at the dust formation sites (Figure 9) using pH strips. Multiple measurements were taken to provide an average pH value for the site of interest and averaged. From these studies, it was noted that the pH was fairly consistently acidic across all samples, as expected. However, we note that the average pH value of the E9 site was marginally higher, whilst that of the E17 site was more acidic than those determined for the other samples (Table 3).

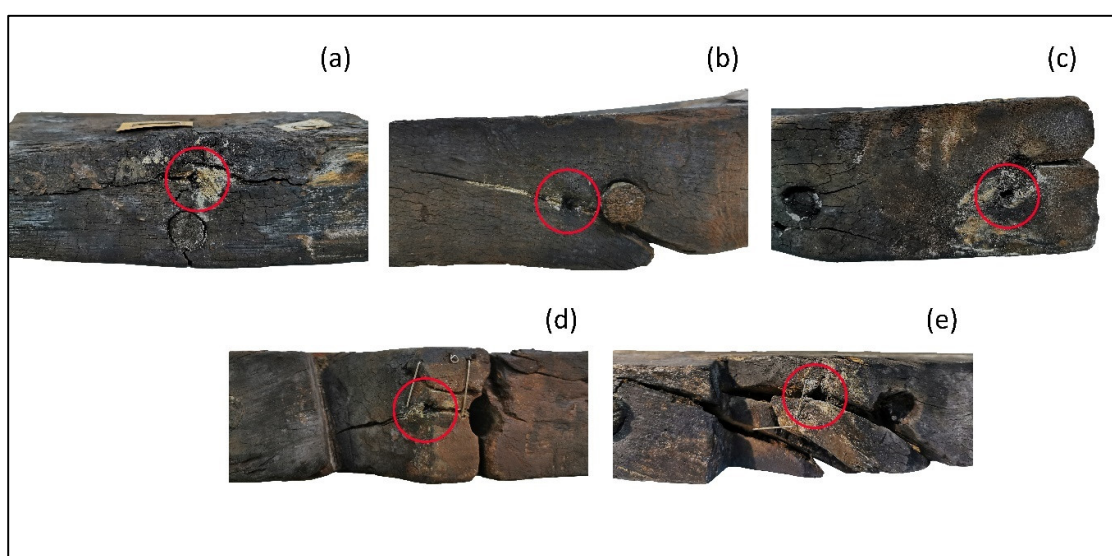


**Figure 9.** Photographs taken to illustrate the areas where pH values were measured for (a) E8, (b) E9, (c) E11, (d) E13, and (e) E17.

**Table 3.** Average pH values determined for the wood samples E8, E9, E11, E13, and E17.

Sample	Average pH
E8	5
E9	6
E11	4
E13	4
E17	3

#### 4. Conclusions

The IU Yenikapı Shipwreck Project is a significant archaeological group within water-logged archaeological wood conservation studies. This is primarily due to the high number of shipwrecks recovered and the various wood species used to construct individual crafts. Whilst conservation studies of the Yenikapı shipwrecks have already been carried out, it is important to continue to understand the requirements for conservation due to unseen threats, which have been reported in previous studies of conserved marine artefacts and other shipwrecks.

Because the sulfur problem within the timbers of shipwrecks whose conservation was completed with PEG is well known, the Yenikapı shipwrecks were monitored during storage. Dust formation was observed when monitoring the woods of the YK 12 shipwreck.

In this study, the dust that occurred in the woods of the YK 12 shipwreck was investigated. First, FTIR and XRD analyses were compared to determine the composition and to explore whether these samples contained sulfur-based salts, wooden parts (such as lignin), and PEG. Firstly, the FTIR spectra of dust samples, PEG, and wood samples, taken where the dust occurred, were evaluated. These results show that all dust samples contained components from wood and PEG. When the spectra of the wood samples, fresh wood samples, and PEG were analysed, it was determined that all the wood samples were impregnated with PEG. Furthermore, a comparison with fresh wood samples (oak, walnut, and hornbeam) demonstrated that hemicelluloses in the E8, E9, E11, and E17 samples degraded. On the other hand, lignin in these samples was less degraded in comparison, with the exception of the E9 wood sample. Kılıç calculated the maximum water content of the waterlogged archaeological woods of the YK 12 shipwreck between 500% and 1000% before the PEG impregnation process [35]. Therefore, the woods of the YK 12 could be classified as Class I, highly degraded [46].

In addition to FTIR analyses, XRD analysis was performed on dust samples collected at various sites. Previous studies in this area showed XRD analysis could reveal the presence of salts in the woods that may have precipitated during drying [44]. All samples contained melanterite ( $\text{FeSO}_4 \cdot 7\text{H}_2\text{O}$ ). Additionally, all samples, except E9, contained rozenite. In contrast, E9 contained quartz. These XRD results were to be expected when compared with the results obtained from other shipwrecks treated with PEG. In particular, these compounds were also found in the wood of Vasa, Mary Rose, Batavia, and Shinan shipwrecks. For instance, an analysis of samples from the Mary Rose revealed that the sulfides had oxidized mainly to rozenite. Many problems can appear due to the occurrence of iron sulfates in the wood. Firstly, this can lead to damaging dust formation on the surface of the wood. Furthermore, the growth of the crystals within the wood causes mechanical stresses that lead to cracks and embrittlement of the organic matter, ultimately destroying the artefact [39].

Another problem linked to the oxidation of iron sulfides is the acidification of the wood. Acidity is harmful to the mechanical resistance of the wood. In addition, acidic conditions can cause the hydrolysis of cellulose and hemicellulose [24]. Acidity formation was detected in the woods of E17. In addition, the pH values of the woods of E11 and E13 confirmed the acidity in these findings. It showed that mechanical resistance problems could appear in the woods of YK 12. Therefore, it is important to monitor the woods and the ambient conditions of the storage area. High relative humidity in the storage area could escalate the acidity problem. Moreover, it may be necessary to treat the woods using neutralization solutions with continued monitoring of the YK 12 shipwreck woods to continue to protect the integrity of the shipwreck after assembling the woods of YK 12.

**Author Contributions:** Conceptualization, A.G.K. and N.K.; Methodology, A.G.K., N.K. and D.C.A.; Writing—original draft, A.G.K. and N.K.; Writing—review & editing, A.G.K., N.K. and D.C.A. All authors have read and agreed to the published version of the manuscript.

**Funding:** This study was funded by the Scientific Research Projects Coordination Unit of Istanbul University. Project number: 39374.

**Acknowledgments:** The authors acknowledge Ufuk Kocabaş, Istanbul Archaeology Museums, Yenikapı Shipwrecks Project Team, and the Scientific and Technological Research Council of Turkey (TUBITAK) for their help and support.

**Conflicts of Interest:** The authors declare no conflict of interest.

## References

1. Braovac, S.; Kutzke, H. The Presence of Sulfuric Acid in Alum-Conserved Wood—Origin and Consequences. *J. Cult. Herit.* **2012**, *13*, S203–S208. [[CrossRef](#)]
2. Broda, M.; Yelle, D.J. Reactivity of Waterlogged Archeological Elm Wood with Organosilicon Compounds Applied as Wood Consolidants: 2D 1H–13C Solution-State NMR Studies. *Molecules* **2022**, *27*, 3407. [[CrossRef](#)]

3. Fix, P.D. Archaeological Watercraft: A Review and Critical Analysis of the Practice. Ph.D. Thesis, Texas A&M University, College Station, TX, USA, 2015.
4. Elding, L.I. Ten years of Vasa research—review and outlook. In Proceedings of the International Conference Shipwrecks 2011, Stockholm, Sweden, 18–21 October 2011; pp. 86–93.
5. Godfrey, I.M.; Richards, V.; Cha, M. The post-treatment deterioration of marine archaeological wood—where to now? In Proceedings of the Asia-Pacific Regional Conference on Underwater Cultural Heritage, Manila, Philippines, 8–12 November 2011; pp. 697–713.
6. Fors, Y. Sulfur-Related Conservation Concerns in Marine Archaeological Wood: The Origin, Speciation and Distribution of Accumulated Sulfur with Some Remedies for the Vasa. Ph.D. Thesis, Stockholm University, Stockholm, Sweden, 2008.
7. Håfors, B. Conservation of the Wood of the Swedish Warship Vasa of AD 1628. Evaluation of Polyethylene Glycol Conservation Programmes. Ph.D. Thesis, University of Gothenburg, Gothenburg, Sweden, 2010.
8. Broda, M.; Hill, C.A. Conservation of waterlogged wood—Past, present and future perspectives. *Forests* **2021**, *12*, 1193. [[CrossRef](#)]
9. Monachon, M.; Albelda-Berenguer, M.; Pele, C.; Cornet, E.; Guilminot, E.; Remazeilles, C.; Joseph, E. Characterization of Model Samples Simulating Degradation Processes Induced by Iron and Sulfur Species on Waterlogged Wood. *Microchem. J.* **2020**, *155*, 104756. [[CrossRef](#)]
10. Sandström, M.; Jalievand, F.; Damian, E.; Fors, Y.; Gelius, U.; Jones, M.; Salome, M. Sulfur accumulation in the timbers of King Henry VIII's warship Mary Rose: A pathway in the sulfur cycle of conservation concern. *Proc. Natl. Acad. Sci. USA* **2005**, *102*, 14165–14170. [[CrossRef](#)] [[PubMed](#)]
11. Almkvist, G.; Persson, I. Fenton-induced degradation of polyethylene glycol and oak holocellulose. A model experiment in comparison to changes observed in conserved waterlogged wood. *Holzforschung* **2008**, *62*, 704–708. [[CrossRef](#)]
12. Fors, Y.; Nilsson, T.; Risberg, E.D.; Sandström, M.; Torssander, P. Sulfur Accumulation in Pinewood (*Pinus Sylvestris*) Induced by Bacteria in a Simulated Seabed Environment: Implications for Marine Archaeological Wood and Fossil Fuels. *Int. Biodeterior. Biodegrad.* **2008**, *62*, 336–347. [[CrossRef](#)]
13. Kılıç, A.G. Sulphur and Iron Analysis Together with Their Distribution in Woods and Their Removal from the Woods of Yenikapı Shipwrecks. Ph.D. Thesis, İstanbul University, İstanbul, Turkish, 2017.
14. Rémazeilles, C.; Saheb, M.; Neff, D.; Guilminot, E.; Tran, K.; Bourdoiseau, J.A.; Refait, P. Microbiologically influenced corrosion of archaeological artefacts: Characterisation of iron (II) sulfides by Raman spectroscopy. *J. Raman Spectrosc.* **2010**, *41*, 1425–1433. [[CrossRef](#)]
15. Kılıç, N.; Kılıç, A.G. Analysis of Waterlogged Woods: Example of Yenikapı Shipwreck. *Art-Sanat* **2018**, *9*, 1–11.
16. Remazeilles, C.; Leveque, F.; Minjacq, M.; Refait, P.; Sanchez, C.; Jézégou, M.P. Characterisation of iron (II) sulfides in wet archaeological woods: The wreck of Mandirac (IV) th century, antique ports of Narbonne, France. In Proceedings of the 13th ICOM-CC Group on Wet Organic Archaeol. Materials Conference, Florence, Italy, 16–21 May 2016.
17. Kılıç, A.G.; Kılıç, N.; Akgün, C. The Importance of Using Multiple Analyses Techniques to Determine the Physical Condition of the Waterlogged Wood. *Wood Res.* **2021**, *66*, 1046–1054. [[CrossRef](#)]
18. Remazeilles, C.; Leveque, F.; Conforto, E.; Meunier, L.; Refait, P. Contribution of magnetic measurement methods to the analysis of iron sulfides in archaeological waterlogged wood iron assemblies. *J. Microchem.* **2019**, *148*, 10–20. [[CrossRef](#)]
19. Almkvist, G.; Persson, I. Distribution of iron and sulfur and their speciation in relation to degradation processes in wood from the Swedish warship Vasa. *New J. Chem.* **2011**, *35*, 1491–1502. [[CrossRef](#)]
20. Smith, A.D.; Jones, M.; Berko, A.; Chadwick, A.V.; Newport, R.J.; Skinner, T.; Salomé, M.; Frederick, J.; Mosselmans, W. An investigation of the Sulfur–Iron chemistry in timbers of the sixteenth century warship, the Mary Rose, by Synchrotron micro-X-ray spectroscopy. In Proceedings of the 37th International Symposium Archaeometry, Siena, Italy, 13–16 May 2008; Turbanti-Memmi, I., Ed.; pp. 389–394. [[CrossRef](#)]
21. Kılıç, A.G. Sulfur Problem in the Conservation of Waterlogged Wood. *TINA* **2020**, *13*, 133–146.
22. MacLeod, I.D. Conservation of waterlogged timbers from the Batavia 1629. *Bull. Aust. Inst. Marit. Archaeol.* **1990**, *14*, 1–8.
23. Zhang, H.; Shen, D.; Zhang, Z.; Ma, Q. Characterization of degradation and iron deposits of the wood of Nanhai I shipwreck. *Herit. Sci.* **2022**, *10*, 1–13. [[CrossRef](#)]
24. Rémazeilles, C.; Meunier, L.; Lévêque, F.; Plasson, N.; Conforto, E.; Crouzet, M.; Refait, P.; Caillat, L. Post-treatment study of Iron/Sulfur-containing compounds in the wreck of Lyon Saint-Georges 4 (Second Century ACE). *Stud. Conserv.* **2019**, *65*, 28–36. [[CrossRef](#)]
25. Sandström, M.; Jalievand, F.; Persson, I.; Gelius, U.; Frank, P.; Hall-Roth, I. Deterioration of the seventeenth-century warship Vasa by internal formation of sulphuric acid. *Nature* **2002**, *415*, 893–897. [[CrossRef](#)]
26. Cha, M.Y.; Godfrey, I.; Richards, V.; Kasi, K.; Byrne, L. Analysis and Deacidification of Acid-Affected PEG Treated Timbers From the Korean Shinan Ship. In Proceedings of the 12th ICOM-CC Wet Organic Archaeological Materials Conference, İstanbul, Turkey, 13–17 May 2013.
27. Seojin, K.; Eung-ho, K.; Yu-na, L. Effect of the Acid Degradation of the Shinan Shipwreck on Indoor Air Quality in the Korean National Maritime Museum. *Stud. Conser.* **2021**, *66*, 272–281. [[CrossRef](#)]
28. Kılıç, A.G. Monitoring of the Conserved YK1 Shipwreck During Storage. In Proceedings of the Symposium on Restoration and Conservation of Traditional Timber Structures 7, İstanbul, Turkey, 2019.

29. Fors, Y. What Happens in the Museum Environment? Post-Conservation Challenges in the Vasa and the Mary Rose. In *Conserving Wrecks for Future Generations, Antarctica Symposium and Workshop*; Hasselt University: Hasselt, Belgium, 2009.
30. Fors, Y.; Grudd, H.; Rindby, A.; Jalilehvand, F.; Sandström, M.; Cato, I.; Bornmalm, L. Sulfur and iron accumulation in three marine-archaeological shipwrecks in the Baltic Sea: The Ghost, the Crown and the Sword. *Sci. Rep.* **2014**, *4*, 4222. [[CrossRef](#)]
31. Kim, S.; Park, W.J. Characteristics of Emission Substances by Acid degradation of Shinan Wreck, Republic of Korea. *Int. J. Conserv. Sci.* **2020**, *11*, 75–86.
32. Kocabaş, U. The Yenikapı Byzantine-Era Shipwrecks, Istanbul, Turkey: A preliminary report and inventory of the 27 wrecks studied by Istanbul University. *Int. J. Nautical Archaeol.* **2015**, *44*, 5–38. [[CrossRef](#)]
33. Özsait-Kocabaş, I. The Yenikapı 12 Shipwreck, a 9th-Century Merchantman from the Theodosian Harbour in Istanbul, Turkey: Construction and reconstruction. *Int. J. Naut. Archaeol.* **2018**, *47*, 357–390. [[CrossRef](#)]
34. Özsait-Kocabaş, I. *Yenikapı 12 An Early Medieval Merchantman*; Ege Publishing: Istanbul, Turkey, 2022.
35. Kılıç, N. Assessment of Pre-Impregnation with Polyethylene Glycol and Vacuum Freeze Drying Method for the Conservation of Yenikapı Shipwrecks. Ph.D. Thesis, İstanbul University, Istanbul, Turkish, 2017.
36. Łucejko, J.J.; McQueen, C.M.A.; Sahlstedt, M.; Modugno, F.; Colombini, M.P.; Braovac, S. Comparative chemical investigations of alum treated archaeological wood from various museum collections. *Herit. Sci.* **2021**, *9*, 69. [[CrossRef](#)]
37. Tran, K. Various Physical and Analytical Methods to Control the Impregnation Efficiency of Archaeological Artefacts by Different Consolidating Resins. In *Proceedings of the Wood Science for Conservation of Cultural Heritage*, Florence, Italy, 8–10 November 2007; Uzielli, L., Ed.; pp. 86–92.
38. Mortensen, N.M. Stabilization of Polyethylene Glycol in Archaeological Wood. Ph.D. Thesis, Technical University of Denmark, Lyngby, Denmark, 2009.
39. Fors, Y.; Jalilehvand, F.; Sandström, M. Analytical aspects of waterlogged wood in historical shipwrecks. *Anal. Sci.* **2011**, *27*, 785. [[CrossRef](#)]
40. Kubovský, I.; Kačíková, D.; Kačík, F. Structural changes of oak wood main components caused by thermal modification. *Polymers* **2020**, *12*, 485. [[CrossRef](#)]
41. Zborowska, M.; Stachowiak-Wencek, A.; Waliszewska, B.; Prądzyński, W. Colourimetric and FT-IR ATR spectroscopy studies of degradative effects of ultraviolet light on the surface of exotic ipe (*Tabebuia* sp.) wood. *Cellul. Chem. Technol.* **2016**, *50*, 71–76.
42. Jiang, Z.; Yi, J.; Li, J.; He, T.; Hu, C. Promoting effect of sodium chloride on the solubilization and depolymerization of cellulose from raw biomass materials in water. *ChemSusChem* **2015**, *8*, 1901–1907. [[CrossRef](#)]
43. Rémazeilles, C.; Tran, K.; Guilminot, E.; Conforto, E.; Refait, P. Study of Fe (II) sulphides in waterlogged archaeological wood. *Stud. Conser.* **2013**, *58*, 297–307. [[CrossRef](#)]
44. Sandström, M.; Fors, Y.; Jalilehvand, F.; Damian, E.; Gelius, U. Analyses of sulfur and iron in marine-archaeological wood. In *Proceedings of the Ninth ICOM Group on Wet Organic Archaeological Materials Conference*, Copenhagen, Denmark, 7–11 June 2004; pp. 181–199.
45. Almkvist, G.; Persson, I. Extraction of iron compounds from wood from the Vasa. *Holzforschung* **2006**, *60*, 678–684. [[CrossRef](#)]
46. Hamilton, D.L. *Methods of Conserving Archaeological Material from Underwater Sites*, Conservation of Cultural Resources I 1999, Nautical Archaeology Program, Texas A&M University. 1999. Available online: <http://nautarch.tamu.edu/class/ANTH605> (accessed on 27 January 2023).

**Disclaimer/Publisher’s Note:** The statements, opinions and data contained in all publications are solely those of the individual author(s) and contributor(s) and not of MDPI and/or the editor(s). MDPI and/or the editor(s) disclaim responsibility for any injury to people or property resulting from any ideas, methods, instructions or products referred to in the content.